Flux trapping in niobium cavities during breakdown events*

J. Knobloch and H. Padamsee
Floyd R. Newman Laboratory of Nuclear Studies
Cornell University, Ithaca, New York 14853

Abstract

We report on the discovery of increased residual losses in niobium cavities following rapid quenches, in particular after thermal breakdown and multipacting. Increases of the residual resistance in the breakdown affected region by more than a factor of 10 have been recorded in some instances. It is believed that magnetic flux, generated by thermocurrents during breakdown, is trapped as the cavity reverts to the superconducting state, resulting in the enhanced losses. A thermal cycle to above the critical temperature of niobium is required to restore the initial low-loss state.

1 Introduction

It is common practice to shield superconducting niobium rf cavities from the earth's magnetic field using mu-metal. This precaution is necessary to prevent the trapping of magnetic flux by pinning centers in the niobium as the cavity is cooled through the transition temperature (T_c). It is well known that any flux remaining in the material is responsible for an additional residual resistance. [1–3] Measurements on 1.5-GHz cavities performed at Saclay have shown that almost all flux present in the cavity wall above T_c is trapped when the cavity is cooled, resulting in a residual resistance of about 350 nΩ per Gauss of flux. [4] Thus, to achieve cavity a cavity quality (Q_0) of 10^{10} at 1.5 GHz, the magnetic field in the cryostat may not exceed about 80 mOe.

However, external magnetic fields need not always be the source of trapped flux. Investigations into Nb_3Sn coated niobium cavities as an alternative to niobium, for example, revealed that magnetic flux can be generated by thermocurrents between the layers of dissimilar metals. If the cavity is cooled too rapidly through the critical temperature, a substantial reduction of the cavity Q_0 is observed. [5]

In the course of high-speed, high-sensitivity thermometric studies of thermal breakdown in 1.5-GHz rf cavities, we have now discovered a similar effect in niobium cavities during thermal breakdown.

Thermal breakdown generally results when a highly resistive defect on the rf surface causes a large fraction of the cavity to go normal conducting. However, it can also be initiated by the heat from bombarding field emission electron, by multipacting, or by the power dissipated due to the BCS surface resistance of niobium. [6]

The acquisition of extensive low-field temperature maps prior to and after thermal breakdown events led to our discovery that the *low-field* surface resistance of the breakdown region can change. In most cases substantial increases were recorded. Correspondingly a reduction of the low-field cavity quality was registered. Initially, this effect was attributed to the redistribution of gases during the breakdown event. However, experimental evidence presented below contradicts this hypothesis. Instead, we now believe that strong temperature gradients, created during breakdown events, drive electric currents thereby generating magnetic flux. The flux is trapped when the cavity reverts to the superconducting state at the end of the quench, resulting in an increased surface resistance.

2 Experimental setup

The experimental setup to study 1.5-GHz (L-band) cavities has been described in a number of papers [7–9] and will not be repeated here in detail. The main diagnostic tool is a fixed-array thermometry system comprising 756 thermometers attached to the cavity exterior. The array is capable of mapping the cavity temperature distribution in superfluid helium at 1.6 K. Important to the study of thermal breakdown are the system's short acquisition times for a temperature map (≈ 0.14 s) and its high resolution (as good as 30 μK). These features permit us to capture the transient breakdown events, and to study their effect on the low-field residual

*Supported by the National Science Foundation with supplementary support under the US–Japan Agreement.

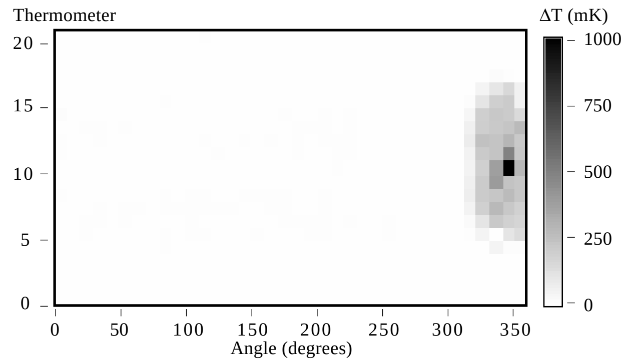

Figure 1: "Flattened" temperature map of defect initiated thermal breakdown in progress in cavity LE1-32. The bottom and top cavity irises are at thermometer 1 and 19, respectively, and the equator is at thermometer 10.

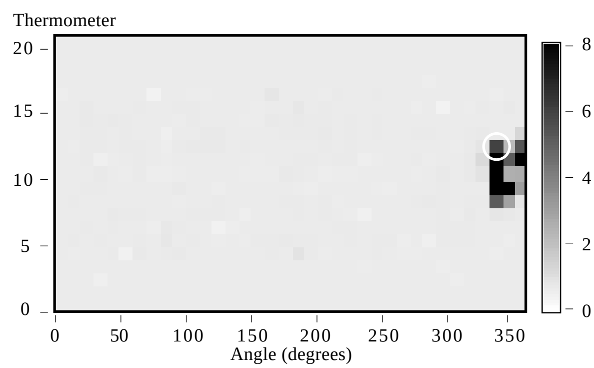

Figure 2: Ratio of the surface resistance (at $E_{\mathrm{pk}} = 10$ MV/m) after several breakdown events in cavity LE1-32 to that before breakdown. Dark regions indicate that the surface resistance increased.

resistance of the cavity. An automated Q_0 versus E_{pk}[1] measurement system operates in conjunction with the thermometry system, to provide information on the integrated cavity losses.

Single-cell cavities of the CEBAF shape were made with RRR = 250 niobium. The cavity preparation prior to testing consisted of a standard chemical treatment [8, 10] (one hour in nitric acid to remove any remaining indium and then about five minutes in buffered chemical polish (BCP 1:1:2)). A rinse with deionized water for one hour followed the chemical etch, before drying the cavity with hot, filtered nitrogen gas and mounting the cavity on the test stand.

3 Modification of the surface resistance

An example of thermal breakdown in progress is shown in Figure 1. This temperature map was obtained by taking numerous maps in succession (≈ 0.14 s apart in time) while thermal breakdown was repeatedly quenching the cavity at $E_{\mathrm{pk}} \approx 20$ MV/m. The origin of the breakdown region was later correlated with the end of the equator weld.

Extensive thermometric data at low electric field was obtained prior to and after the breakdown events. A convenient way of comparing this data, is to take the ratio of the surface resistance. An example is given in Figure 2.

Most of the cavity is unaffected by thermal breakdown. However, the region directly involved in the quench has clearly increased its surface resistance by a substantial amount. The increases recorded were as high as a factor of 16. Figure 3 depicts the changes undergone by one of the affected sites during numerous breakdown events. In particular, we found that multiple breakdown events could result in successively larger R_{s} values, as is revealed by the data obtained during the second series of breakdown events.

[1] E_{pk} is the peak electric field in the cavity.

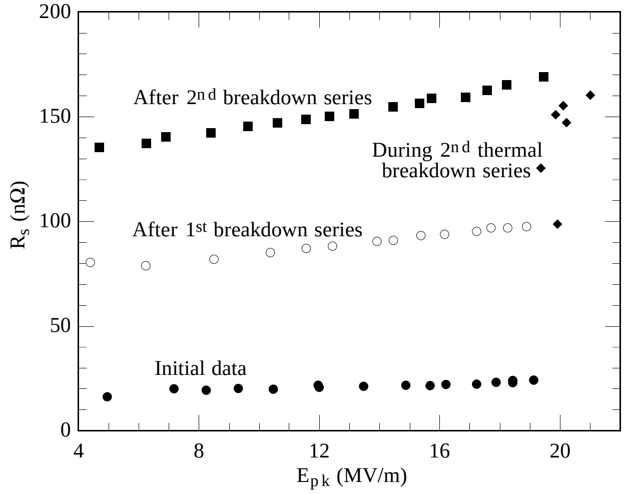

Figure 3: Surface resistance at the circled site in Figure 2 during and following a series of thermal breakdown events in the cavity.

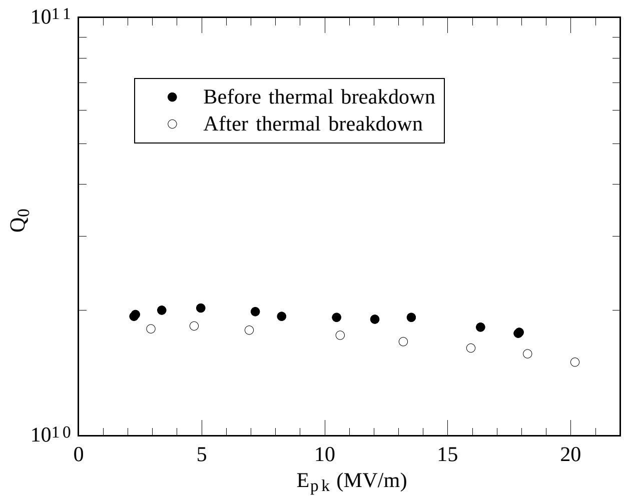

Figure 4: Q_0 versus $E_{\rm pk}$ data obtained from power measurements on cavity LE1-32, prior to and after thermal breakdown events like those in Figure 1.

Prior to any breakdown, the recorded surface resistance at the site in Figure 3 was about 15 nΩ, close to the mean cavity surface resistance of 14 nΩ ($Q_0 = 2 \times 10^{10}$). The total effect of all the breakdown events was to raise the surface resistance by a factor of nine to 135 nΩ! If the entire cavity had been affected in this manner, the Q_0 would have dropped to 2.2×10^9. In fact, only a small fraction of the cavity surface is involved in the process, so that the Q_0 drop is significantly less. Nevertheless a Q_0 degradation was observed, as shown in Figure 4, which corroborates the calorimetric data.

The effect of thermal breakdown on the cavity $R_{\rm s}$ described here was observed in *all* cavities that were limited by thermal breakdown related to cavity defects. In some cases, however, a few sites towards the periphery of the affected region would actually reduce their surface resistance. This effect is attributed to discharge cleaning of the rf surface and is discussed in more detail in another paper. [8, 11]

Whenever we cycled an afflicted cavity to room temperature, the surface resistance of breakdown affected regions would revert to their original values prior to any thermal breakdown. If thermal breakdown was triggered again following the thermal cycle, the $R_{\rm s}$ would increase once more. A second thermal cycle could be used to remove the losses again.

To investigate this effect further, we attached a cryogenic linear temperature sensor (CLTS) to the equator of cavity LE1-32 near the thermal breakdown center in Figure 1. The cavity fields were raised until thermal breakdown was observed. Low-field data prior to and after thermal breakdown confirmed that the $R_{\rm s}$ increased

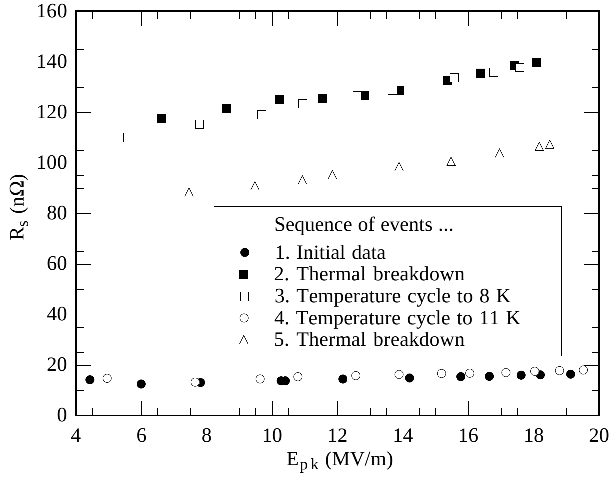

Figure 5: Surface resistance recorded by thermometer 11 at 330° with cavity LE1-32 (just below the circled site in Figure 2). The data was obtained in the following sequence: 1. before any thermal breakdown, 2. following a series thermal breakdown events, 3. following a thermal cycle to 8 K, 4. following a second thermal cycle to 11 K, and 5. following a new series of thermal breakdown events.

as in Figure 2. Liquid helium was then transferred out of the cryostat until the CLTS temperature drifted to a desired value. A retransfer of liquid helium then rapidly cooled the cavity to 4.2 K before we pumped the bath to further lower the temperature to 1.6 K.

A temperature cycle to 8 K had no effect on the cavity surface resistance. Surprisingly, though, upon cycling to 11 K all increased losses reduced back to their original values.[2] These results are shown in Figure 5. Following the temperature cycle to 11 K, the cavity fields were raised once more until thermal breakdown took place, again resulting in increased low-field losses. In many cases (as in Figure 5) the order of magnitude of the increases was the same as previously. However, the actual values were not identical to those observed after the first breakdown sequence.

4 Discussion

Initially we had suspected that gases evolving from the hot defect were being redistributed near the breakdown site, resulting in the increased losses. This hypothesis was however ruled out by the results from the thermal cycles to 8 K and 11 K. Furthermore, this theory is inconsistent with the observation that the increased losses saturate following a few breakdown events, yet after a temperature cycle to 11 K they are reactivated to their full extent by a new series of breakdown events.

Our data suggests that the critical temperature of niobium ($T_c = 9.22$ K) plays an important role in eliminating augmented rf losses. In fact, the losses we observed are reminiscent of a similar effect detected in Nb_3Sn coated niobium cavities. These cavities were investigated because Nb_3Sn has a critical temperature almost twice that of pure niobium (18.2 K). Tests have shown that Q_0 values in excess of 10^{10} can be achieved. [12] Curiously, though, the Q_0 would degrade drastically, falling by more than a factor of two, if the cavity was cooled through 18.2 K at rates exceeding one Kelvin every five minutes. [5]

This result was attributed to currents driven by a strong thermovoltage that is generated between the niobium and Nb_3Sn layers. These currents produce magnetic flux that is trapped if the cavity is cooled too rapidly, resulting in increased losses. [5]

Similar to our observations with niobium cavities, a quench in a Nb_3Sn cavity resulted in increased losses that could only be removed by warming the cavity above T_c and cooling slowly again. The increased losses were also explained by the thermovoltage theory, since the cavity is cooled very rapidly through T_c following thermal breakdown.

In our niobium cavities no two dissimilar metals exist, yet we observe the same (although reduced) effect. Hence, we must consider temperature gradients, rather than thermocouple effects, as the driving force behind

[2]Tests of another cavity showed that regions which reduced their losses were unaffected by a cycle to 12 K, a point discussed in References [8, 11].

the flux generating currents.[3] This phenomenon is known as the *Seeback effect.* [13]

Following thermal breakdown and the collapse of the cavity fields, a centimeter size region surrounding the defect is normal conducting. The cavity then is cooled very rapidly by the helium bath, and calculations show that the normal conducting region shrinks and disappears in as little as a few to 10's of milliseconds. [14, 15] These times are consistent with our observation that two successive temperature maps, taken 0.14 seconds apart, never capture the same thermal breakdown event. Large, radial temperature gradients, that drive the thermocurrents, exist near the rapidly shrinking normal conducting–superconducting boundary. Magnetic flux created by the thermocurrents can be trapped as the niobium reverts to the superconducting state. An increased surface resistance results.

It should be emphasized that there are two important aspects to this flux trapping mechanism: 1. high temperature gradients are essential to create magnetic flux, and 2. rapid temperature changes are needed when cooling through T_c to trap the flux.

The electric field generated by the Seeback effect due to a temperature gradient $\boldsymbol{\nabla} T$ is given by

$$\mathbf{E} = S_T \boldsymbol{\nabla} T, \tag{1}$$

S_T being the thermopower. [13] Studies have shown that the temperature of defects responsible for thermal breakdown can be very elevated with respect to the helium bath. [8] Furthermore, during thermal breakdown, temperatures over a large region easily exceed T_c, as demonstrated by thermometry. Thus, substantial $\boldsymbol{\nabla} T$'s are possible.

Thermopowers vary in sign and magnitude from material to material and are temperature dependent. At room temperature, observed thermopowers for niobium are on the order of microvolts/Kelvin [16], whereas at cryogenic temperatures (near 10 K), values for silver and copper[4] are about 1/10 of a microvolt/Kelvin. [17, 18] The length scale over which temperatures vary during thermal breakdown is set by the size of the breakdown region, which is on the order of a few centimeters. The minimum temperature difference expected over this distance is at least 10 K. Hence the *smallest* temperature gradient to be anticipated is about 2 K/cm. The thermoelectric field developed in this case will be about 0.2 μV/cm. Given a resistivity of 0.062 $\mu\Omega$ cm for $\approx$ 300 RRR niobium at cryogenic temperatures [19], the current density (j_T) driven by the thermogradient is on the order of

$$j_T \approx \frac{0.2\ \mu\text{V/cm}}{0.062\ \mu\Omega\ \text{cm}} = 3\ \text{A/cm}^2. \tag{2}$$

The magnetic fields created by such current densities are on the order of 1.9 Oe at a distance of 1 cm. Past measurements have shown that the sensitivity of R_s to flux trapping is about 0.35 nΩ/mOe. [4] If all of the flux created by thermopower is trapped, R_s changes as high as 660 nΩ should be observed. Considering our lack of concrete data on the actual temperature gradients and thermopowers occurring during thermal breakdown our experimental values agree reasonably well with the estimate.

5 Flux trapping during multipacting

Related thermometric studies have revealed the presence of short-lived two-point multipacting along the cavity equator, starting at 30 MV/m. [20] Simulations that confirm the multipacting, demonstrated that intense electron bombardment occurs with less than a millimeter of the equator leading to a quench (see Figure 6(a).

We found, similar to thermal breakdown due to defects, that multipacting changes the surface resistance along the equator (Figure 6(b)). Primarily, multipacting increases the R_s. This fact is clearly demonstrated by the histograms in Figure 7.

Temperature cycles confirmed that flux trapping is the likely cause of the R_s increases. Since they occurred exclusively along the equator, strong thermal gradients must develop in this region due to the electron bombardment during multipacting.

6 Flux trapping during field emission related breakdown

Unlike the case of thermal breakdown caused by a defect, less severe R_s changes were observed following field emission related breakdown. This fact is also consistent with our theory that flux trapping is responsible for

[3] We should point out, that the shielded earth's magnetic field cannot account for the increased losses, since, in our experiment, it can maximally contribute about 10 nΩ to the surface resistance.

[4] We were unable to find thermopower measurements for niobium at low temperatures.

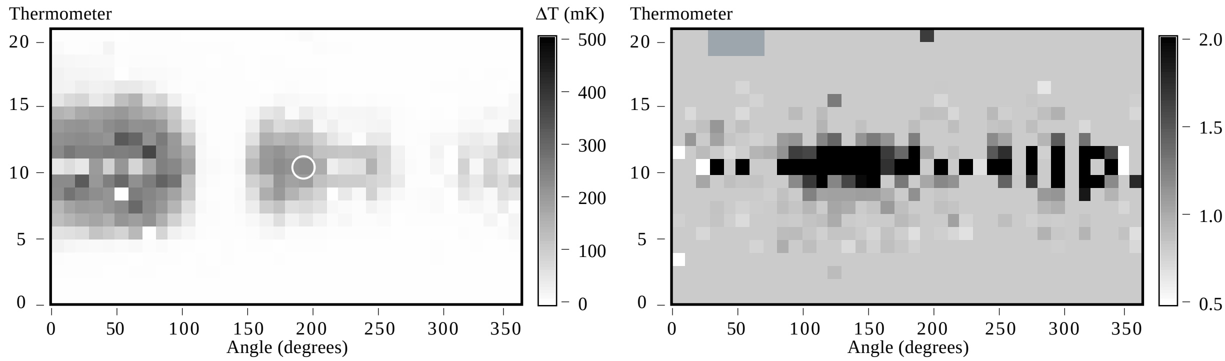

(a) (b)

Figure 6: (a) Temperature map taken during a test of cavity LE1-21 while multipacting was active at $E_{\rm pk} \approx$ 34 MV/m. (b) Ratio of the cavity's surface resistance after and prior to multipacting, depicting increased losses along the equator.

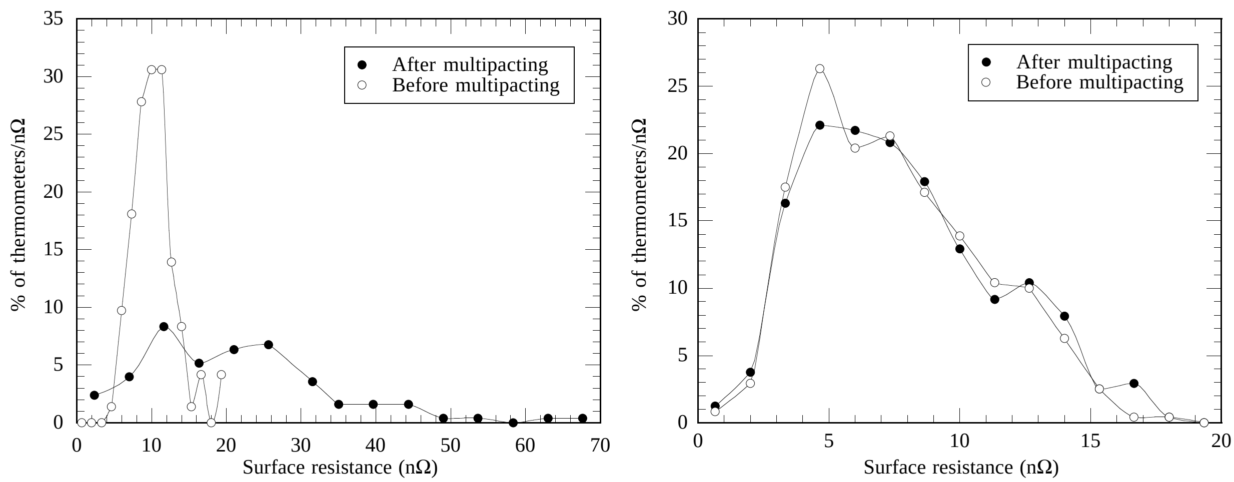

(a) (b)

Figure 7: Histogram of $R_{\rm s}$ of sites in cavity LE1-21 covered by (a) the equator thermometers and their nearest neighbors, and (b) the thermometers away from the equator. In (a) the mean surface resistance increased from 10.3 nΩ to 21.4 nΩ following a series of breakdown events whereas in (b) the mean surface resistance did not change significantly.

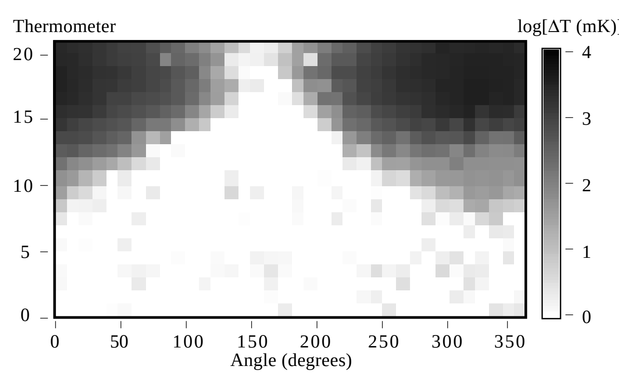

Figure 8: Cavity quench due to inadequate cooling by the helium bath of cavity LE1-33. The bath level at this time was roughly at the height of the equator (thermometer 10). Note the logarithmic temperature scale.

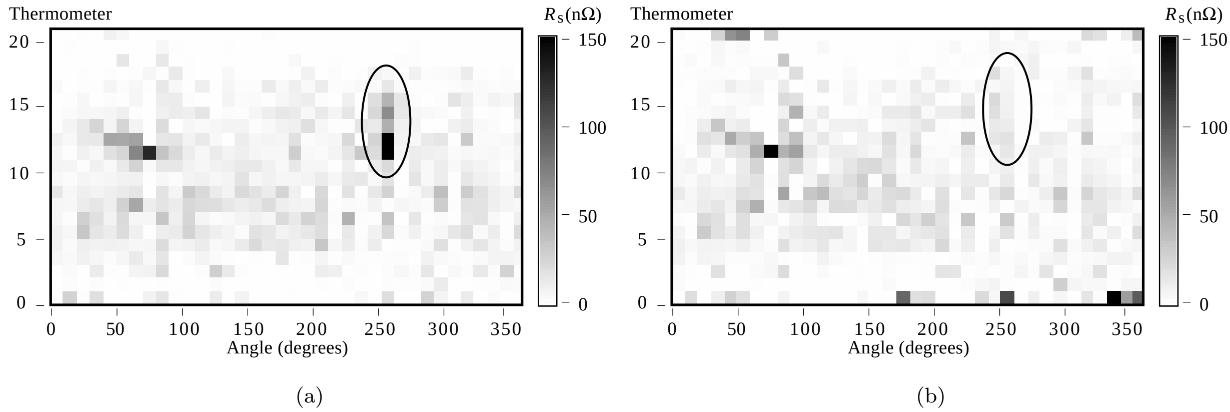

Figure 9: Map of the surface resistance of cavity LE1-33 at $E_{\rm pk} = 12$ MV/m. (a) Before the quench in Figure 8 occurred, and (b) after the quench. The circled region had previously increased its surface resistance due to defect related thermal breakdown.

the $R_{\rm s}$ increases. Defect related thermal breakdown grows from a microscopic region and therefore we expect large thermal gradients. In contrast to this situation, field emission electrons bombard and heat large regions, and less severe temperature gradients are generated when thermal breakdown is initiated. The lack of large gradients explains why the magnetic flux generated is not as substantial as for defect related breakdown.

Similarly, flux trapping and the associated increase in $R_{\rm s}$ does not occur when a cavity quench occurs due to low liquid helium levels. We observed such a breakdown in cavity LE1-33, where almost the entire upper half cell became normal conducting, as shown in Figure 8. In this case, the absence of large thermal gradients is clear. Furthermore, the time it took the cavity to recover from the quench was as long as a few tenths of a second because of poor cooling by the bath, rather than milliseconds during regular thermal breakdown.

By coincidence, defect initiated thermal breakdown had previously occurred in this cavity, and increased $R_{\rm s}$ values were recorded in the region circled in Figure 9(a). Following the quench due to the low liquid helium level, the increased losses disappeared again (see Figure 9(b)).

These observations are entirely consistent with the thermal cycling experiments discussed earlier. The defect initiated thermal breakdown trapped flux in the rf surface, increasing $R_{\rm s}$. Then the quench due to the low helium bath level increased the temperature above $T_{\rm c}$, thereby freeing the flux again. Because of the relatively slow cooling and the absence of large temperature gradients, no new flux was trapped as the cavity cooled, and the original low-$R_{\rm s}$ state was maintained. Evidently subsecond thermal cycles are sufficient to reduce losses, in agreement with the theory that flux trapping is the cause of the high $R_{\rm s}$ regions.

6.1 Summary

The study of thermal breakdown and multipacting led to our discovery of a new loss mechanism. Not only does the breakdown limit the maximum attainable field, but it can also increase the residual resistance in the cavity region directly involved in the breakdown. Increases by over 100 nΩ have been recorded. We believe that magnetic flux, generated by the high temperature gradients during thermal breakdown, is trapped as the cavity wall cools rapidly at the end of the breakdown cycle. A thermal cycle — even if only subsecond in length — to above the critical temperature $T_{\rm c}$ is required to release the flux again.

References

[1] J. Bardeen and M. J. Stephen, *Physical Review* **140**, 1197 (1965).

[2] Y. B. Kim, C. F. Hempstead, and A. R. Strnad, *Physical Review* **139**, 1163 (1965).

[3] J. I. Gittleman and B. Rosenblum, *Journal of Applied Physics* **39**, 2617 (1968).

[4] C. Vallet et al., Flux trapping in superconducting cavities, in *Proceedings of the 1992 European Particle Accelerator Conference*, edited by H. Henke, H. Homeyer, and C. Petit-Jean-Genaz, pages 1295–1297, Berlin, Germany, 1992.

[5] M. Peiniger et al., Work on Nb_3Sn cavities at Wuppertal, in *Proceedings of the 3rd Workshop on RF Superconductivity*, pages 503–531, Argonne, 1987, Proceedings also published as internal Argonne report ANL-PHY-88-1.

[6] H. Padamsee, J. Knobloch, and T. Hays, *RF Superconductivity for Accelerators*, Wiley and Sons, New York, 1998, To be published.

[7] J. Knobloch, H. Muller, and H. Padamsee, *Review of Scientific Instruments* **65**, 3521 (1994).

[8] J. Knobloch, *Advanced Thermometry Studies of Superconducting RF Cavities*, PhD thesis, Cornell University, 1997, Laboratory of Nuclear Studies thesis CLNS 97-3.

[9] J. Knobloch and H. Padamsee, *Particle Accelerators* **53**, 53 (1996), Also published in the Proceedings of the 7th Workshop on RF Superconductivity, Gif-sur-Yvette, France, pp. 95–103 (1995).

[10] P. Kneisel, Surface preparation of niobium, in *Proceedings of the Workshop on RF Superconductivity*, edited by M. Kuntze, pages 27–40, Karlsruhe, 1980, Proceedings also published as internal Kernforschungszentrum Kalsruhe report KFK-3019.

[11] J. Knobloch and H. Padamsee, Reduction of the surface resistance in superconducting cavities due to gas discharge, in *Proceedings of the 8th Workshop on RF Superconductivity*, Padua, Italy, 1997.

[12] G. Müller et al., Nb_3Sn layers on high-purity Nb cavities with very high quality factors and accelerating gradients, in *Proceedings of the 1996 European Particle Accelerator Conference*, edited by S. Myers, A. Pacheco, R. Pascual, C. Petit-Jean-Genaz, and J. Poole, pages 2085–2087, Barcelona, Spain, 1996.

[13] N. Ashcroft and D. Mermin, *Solid State Physics*, W. B. Saunders, 1976.

[14] T. Hays, (Cornell University) Private communication.

[15] M. Pekeler, *Untersuchungen der Feldbegrenzenden Mechanismen in Supraleitenden Niob-Resonatoren*, PhD thesis, Deutsches Electronen-Synchrotron (DESY), 1996.

[16] V. Raag and H. V. Kowger, *Journal of Applied Physics* **36**, 2045 (1965).

[17] E. R. Rumbo, *Journal of Physics F* **6**, 85 (1976).

[18] A. M. Guenault and D. G. Hawksworth, *Journal of Physics F* **7**, L219 (1977).

[19] J.-M. Abraham, C. Tete, and B. Deviot, *Journal of the Less Common Metals* **37**, 181 (1974).

[20] J. Knobloch and H. Padamsee, Multipacting in 1.5-GHz superconducting niobium cavities of the CEBAF shape, in *Proceedings of the 8th Workshop on RF Superconductivity*, Padua, Italy, 1997.